



Next Generation Very Large Array Memo No. 80

Quasar Wind SZ imaging with the ngVLA

C.L. Carilli, M. Lacy, B. Mason (NRAO)
A. Chakraborty, S. Chatterjee (Presidency University)

Abstract

We investigate the ability of the ngVLA reference configuration to image the Sunyaev-Zeldovich effect associated with winds from quasars (and strong starbursts). We employ both a high and low mass black hole model at $z = 1$. We find that the ngVLA core is significantly more sensitive on arcsecond scales than the matching resolution configurations of ALMA and the VLA at 100 GHz and 34 GHz, respectively. The ngVLA will image kpc-scale structures in the winds with high fidelity. However, the short spacing limits in all cases (except the SBA), are such that diffuse emission on scales $> 10''$ is incompletely restored in the images.

1 Introduction

Lacy et al. (2018a) have opened up the new field of imaging the strong winds associated with luminous quasars and starbursts at high redshift through their effect on the temperature of the CMB. Analogous to the SZ effect due to hot cluster gas, Thomson scattering by the free electrons exchanges energy between the CMB photon field and the gas, and shifts the temperature of transmitted photon field, leading to temperature decrements or increments, depending on the temperature and bulk motion of gas (thermal and kinetic SZ). However, unlike the cluster SZ effect, winds associated with quasars and starburst galaxies, will appear on smaller scales, comparable to galaxies (few to tens of kpc).

Details of the physical processes involved can be found in Lacy et al. (2018b). In this memo, we investigate the capability of the ngVLA to image the SZ signature from quasar and starbursts winds at high redshift.

We adopt two models, generated originally by Khandai et al (2015), corresponding to the expected winds from a luminous and faint AGN at $z = 1$. We employ the ngVLA core array, and the Small Baseline Array. We then compare the results to those expected for VLA and ALMA configurations with matched resolution to the ngVLA core.

The primary goals of this study are to:

- Quantify the differences in capabilities of the ngVLA, ALMA, VLA, at match resolution, for quasar SZ studies.
- Investigate the ability of the ngVLA to image fainter, small scale structure.
- Determine how well the core can restore large structures, relative to the SBA.
- Determine the accuracy with which the ngVLA can recover the spectrum between 34 GHz and 100 GHz.

2 Sky and Telescope Models, and Simulations

The models were selected from the cosmological simulations of Kandai et al (2015) (see also Chowdhury et al. 2020), based on an extension of the GADGET2 and GADGET3 Tree Particle Mesh-Smoothed Particle Hydrodynamics code. Both simulations have dark matter and gas dynamics. The simulations also include radiative gas cooling, star formation, black hole growth and feedback. Two regions of the simulation at $z = 1$ were chosen, one with a black hole mass of $7.5 \times 10^7 M_\odot$, and one with a mass of $1.49 \times 10^9 M_\odot$, with corresponding luminosities when accreting at the Eddington limit of $2.4 \times 10^{12} L_\odot$ and $4.8 \times 10^{13} L_\odot$, respectively. We calculate models at 100 GHz and 34 GHz. We note that diffuse signal extends to the edge of the model field of view of ($36''$).

We employ the ngVLA Rev C Core configuration (Selina et al. 2018). The configuration has 94 antennas of 18m diameter in the Core. This array is chosen to provide adequate resolution, down to $0.4'' = 3\text{kpc}$ at 100 GHz, to image the small scale structure. The maximum and minimum baselines for all the arrays are given in Table 1.

We also investigate sensitivity to the larger scale, fainter, halos of the galaxies, on scales up to $\sim 36''$, which is the field size of the input models, using the core and the SBA. The SBA has 19 antennas of 6m diameter, in a compact configuration.

The sky models and telescope model are folded through the SIMOBSERVE process as described in Carilli et al. (2017). We then insert noise per visibility using the setnoise tool in CASA. We adopt a noise value based on the Rev C system parameters, assuming a bandwidth of 10 GHz for the ngVLA. We assume a 4 hour observation.

For comparison, we employ the ALMA C5 configuration at 100 GHz, which has a maximum baseline of 1.3 km, similar to the ngVLA core. We also consider the JVLA-D configuration at 34 GHz, which has a maximum baseline of 1 km. We add noise as per the exposure calculators. For the ALMA models, we adjust the declination of the model to -30° . We use 8 GHz bandwidth for ALMA and the JVLA.

For the imaging, we employ TCLEAN, with a $\sim 0.1''$ cell size, and an image size of 500 to 1000 pixels. Note that the input model images have a field size of $36''$, and faint emission extends to the edge of the fields in the models. We employ Briggs weighting with $R=2$ and $R=-0.5$ for the ngVLA core, to explore capabilities at different resolutions. For the SBA, ALMA, and JVLA, we use $R=2$. In all cases, we use a multiscale clean with scales $[0,7,25]$, and we clean to the 1σ noise level. The resulting resolutions and image noise values are given in Table 1.

3 Results

3.1 Images

Figure 1 shows the ngVLA and ALMA 100 GHz images, with $R=2$ for the bright model (higher black hole mass). Overlaid, in all cases, are contours of the input model without noise. The resolutions are $0.6''$ and $0.7''$, respectively. While the noise in the ngVLA is lower than the ALMA image by a factor of almost 4, generally, both images pick up the brighter emission regions from the main galaxy. The ngVLA image does detect more of the compact 'knots' of emission, corresponding to density clumps in the galaxy halo. However, in both cases, the images only restore about 30% of the total flux density in the model, due to incomplete short spacing coverage. We return to this point below.

Figure 2 shows the ngVLA using $R=-0.5$ for the bright model, which gives higher resolution ($0.38''$), and higher noise, by a factor 2. At high resolution, the ngVLA reveals the small scale structure in the quasar wind, corresponding to local density enhancements, and shocks from recent outflows.

Figure 2 also shows the SBA image. Note, again, that the model field

size is $36''$, while this image field size is somewhat larger. There is diffuse emission in the model that extends to the edge of model field – the edge of the model field can be seen as an edge in the contours in the northern part of the field. The SBA gives a resolution of $11''$, and recovers most of the total flux density (see below).

The power of the ngVLA comes with the high resolution imaging of the fainter model. This model has is almost 30 times fainter than the bright model. Figure 3 shows the faint source ngVLA image at $0.6''$ resolution, plus model contours. The prominent ring is seen in some detail, including some of the fainter extensions. The ring corresponds to an expanding shock associated with a recent phase of quasar activity. Figure 4a shows the corresponding ALMA image, in which the brightest parts of the ring appear as three clumps. Figure 4b shows the ngVLA image at $0.38''$ resolution, delineating the fine scale structure around the ring.

Figure 5 shows the images of the bright model at 34 GHz from the ngVLA core and the VLA D configuration, both at $\sim 2''$ resolution. The ngVLA image is substantially more sensitive than the VLA, and the source structure is reasonably recovered out to $\sim 8''$ radius. The VLA image certainly detects the source, but the structure is noisy.

Figure 6 shows the ratio between 100 GHz and 34 GHz, calculated by smoothing the ngVLA 100 GHz image to the 34 GHz resolution. The expected ratio of ~ 30 , is recovered in the brightest regions of the source, but the ratio decreases toward the source extremities. This decrease is due to the fact that the 100 GHz image using the Core lacks spacings short enough to recover the more diffuse emission (see below), while the lower frequency data performs better in this regard.

3.2 Restoring total flux density

An important question for studies of the SZ effect, and diffuse emission in general is: how well does the configuration restore the larger scale emission? We address this by looking at the total flux densities in the final images and the uv-data, compared to the model. The complication, in this case, is that the ngVLA has an 18m diameter antenna, the VLA a 25m antenna, ALMA a 12m antenna, and the SBA a 6m antenna. Hence, the apparent source brightness distribution, meaning the source as seen by the array, needs to be weighted by the power pattern of the primary beam in each case before comparison. SIMOBSERVE performs such a weighting prior to calculating visibilities, and we have done so for the model images in order to determine the fraction of restored flux.

Table 2 summarizes the results. In the table, we include total flux densities in the input models, the primary beam weighted models, and then in the interferometric images and the peak amplitudes on the shortest baselines of the uv-data. We also show in Figure 6 and 7 plots of the uv data amplitudes vs. baseline length for the different arrays.

For the bright model at 100 GHz, the ngVLA and ALMA both miss most of the total flux density in the model, restoring about 1/3 of the total. The shortest uv-spacings of the ngVLA also only see 1/3 of the total. For ALMA, there are two short baselines that see 70% of the total flux density, but apparently these two baselines are not enough to restore the extended emission in the image. The story is similar, but not as extreme, for the faint source model. The faint model has more flux density on smaller angular scales.

For comparison, the SBA recovers about 90% of the total flux density in the image and uv-data for the bright model.

At 34 GHz, the ngVLA restores 54% of the total flux density in the image. Curiously, even though the VLA has a longer shortest baseline than the ngVLA, the VLA image recovers about 70% of the total. This may reflect the more centrally concentrated, exponential distribution of the antennas along the arms of the VLA, compared to the pseudo-random distribution of antennas in the ngVLA core.

4 Summary

The main results of this study are:

- The ngVLA core sensitivity is 4x better than ALMA, detecting more of the faint knots corresponding to density enhancements in the ambient gas. Generally, images at $\sim 0.7''$ resolution look similar, with the higher sensitivity of the ngVLA offsetting the two shorter baselines afforded by ALMA C5.
- The ngVLA usefulness comes with $R=-0.5$, providing a factor of almost two higher resolution, revealing substructure and shocks on kpc-scales in the winds in the inner parts of the galaxy. This is true even for relatively low mass black hole systems.
- For the ngVLA, the minimum baseline of 30m leads to missing large scale structure on scales $> 10''$, and the total restored flux density is only 1/3 of the total in the model field. The same is true for ALMA,

even though C5 has two baselines down to 15m. Apparently, these two baselines are not enough to properly restore the larger scale structure in the image.

- The SBA restores about 90% of total flux density in the field, but of course does not resolve structure in the galaxy.
- At 34GHz, the ngVLA core goes seven times deeper than the VLA D array. In both cases, about 2/3 of the total flux is restored, but the resolution in both cases is insufficient to delineate structure in the inner galaxy.
- The spectrum between 100 GHz and 34 GHz is recovered only in the brightest emitting regions in the central few arcseconds of the galaxy. The more diffuse emission in the outer regions of the galaxy shows a systematically flatter spectrum (lower ratio of 100 GHz to 34 GHz), since the 100 GHz image is missing more diffuse emission.

Overall, the ngVLA core will be a powerful tool to image SZ structure in quasar and strong starburst winds, on scales of a few arcseconds, or less, such as the substructure in the blast wave or dense clumps in the ISM. However, the 30m minimum baseline implies that more diffuse structures on scales $\sim 10''$ to $15''$, and larger, are not completely restored at 100 GHz. The SBA restores the large scale structure, but does not resolve the sub-structure in the galaxy itself.

References

- Carilli, C. 2017, ngVLA memo 16
Chowdhury et al. 2020, ApJ, 889
Khandai et al 2015, MNRAS, 450, 1349
Lacy et al. 2018a, MNRAS, 483, L22
Lacy et al. 2018b, ASPC, 517, 649
Selina et al. 2018, ASPC, 7, 15

Table 1: Resolution and Sensitivity

Array	Freq GHz	Model	Resol arcsec	RMS μ Jy/bm	B_{min} m	B_{max} m
ngVLA core R=2	100	Bright	0.60''	1.5	28	1300
ngVLA core R=2	100	Faint	0.60''	1.3	28	1300
ngVLA core R=-0.5	100	Bright	0.38''	2.8	28	1300
ngVLA core R=-0.5	100	Faint	0.38''	2.7	28	1300
ngVLA SBA	100	Bright	11''	200	10	55
ALMA C5	100	Bright	0.7''	5.6	15	1350
ALMA C5	100	Faint	0.7''	4.9	15	1350
ngVLA	34	Bright	1.8''	0.5	28	1300
VLA D	34	Bright	2.2''	3.3	40	1000

Table 2: Restoring total flux density

	Bright 100 GHz mJy	Faint 100GHz mJy	Bright 34GHz mJy
S_{mod}	-25.3	-1.0	-0.76
$S_{mod} \times PB_{ngVLA}$	-20.9	-0.91	-0.74
$S_{ngVLA,im}$	-6.4	-0.51	-0.40
$S_{ngVLA,uv}$	-7	-0.85	-0.64
$S_{mod} \times PB_{SBA}$	-25	-0.91	-0.74
$S_{SBA,im}$	-22	–	–
$S_{SBA,uv}$	-23	–	–
$S_{mod} \times PB_{ALMA}$	-23.8	-0.97	–
$S_{ALMA,im}$	-6.0	-0.44	–
$S_{ALMA,uv}$	-16	-0.8	–
$S_{mod} \times PB_{VLA}$	–	–	-0.73
$S_{VLA,im}$	–	–	-0.53
$S_{VLA,uv}$	–	–	-0.6

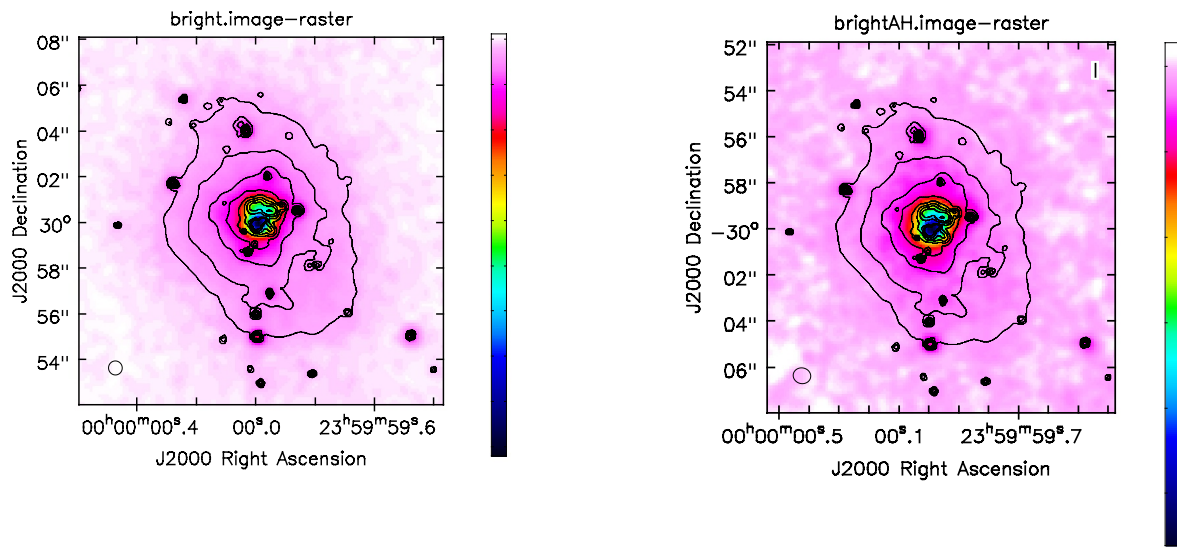


Figure 1: Left: The ngVLA image of the bright model at 100 GHz, 0.60'' resolution (color scale). The contours are for the input model. The color scale ranges from -0.45 to 0 mJy/beam. Right: same, but for the ALMA image at 0.7'' resolution. The color scale ranges from -0.55 to +0.05 mJy/beam. In all images herein, the contours are a geometric progression in square root two. Negative contours are solid, since the signal is negative.

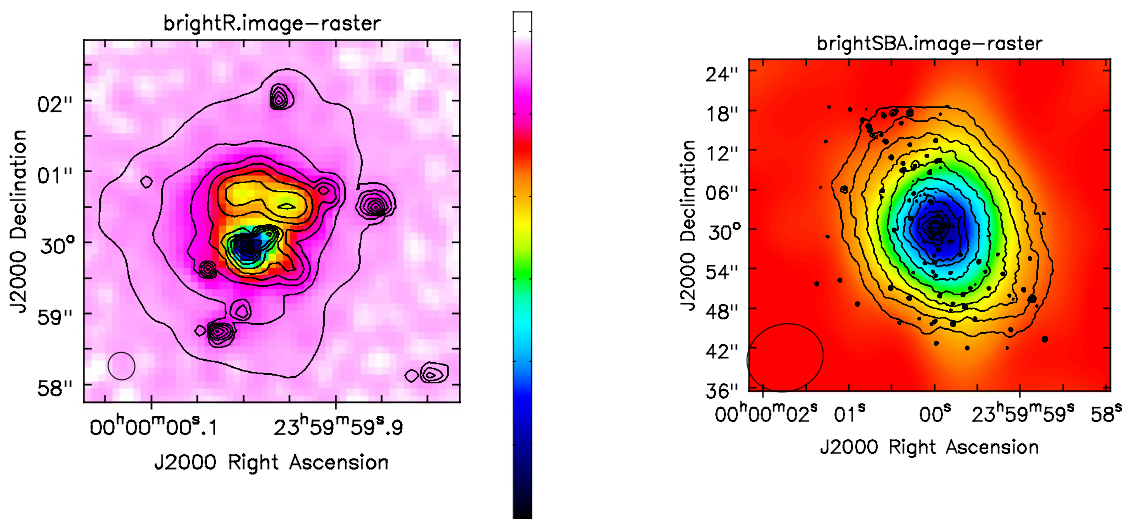


Figure 2: Left: Image of the bright model at 100 GHz, 0.38" resolution (Color scale), plus contours of the input model. The color scale goes from -0.3 to 0 mJy/beam. Right: The SBA image of the bright model, plus contours of the input model on larger scales. The color scale goes from -10 to +2 mJy/beam. Note the straight edge on the contours at the top of the SBA image. This corresponds to the edge of the input model field.

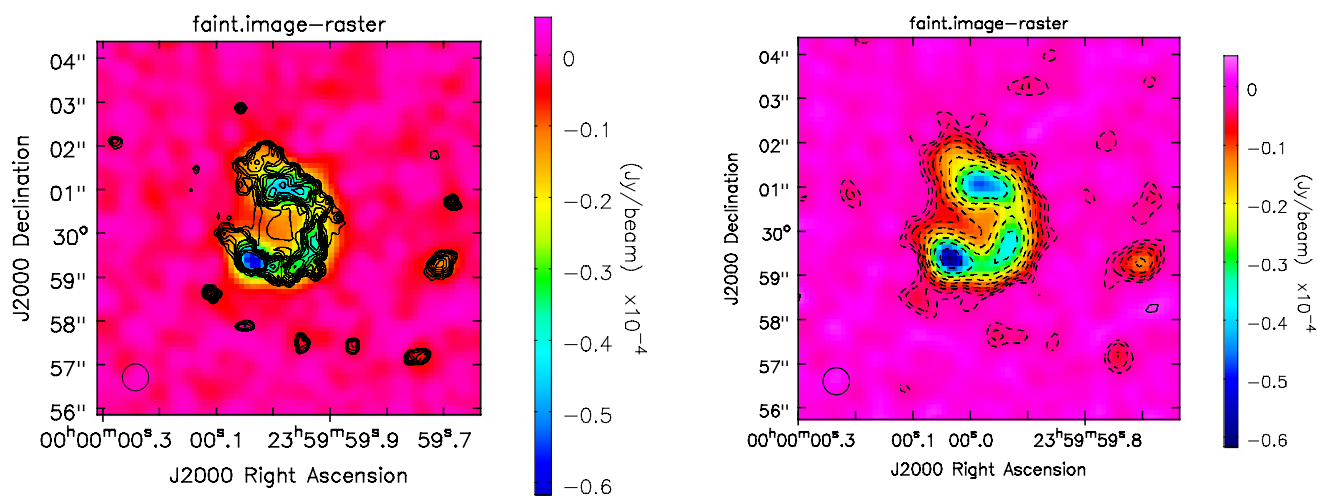


Figure 3: Left: The color shows the ngVLA image at $0.60''$ resolution of the faint model at 100 GHz. The contours are the input model. Right: Both color and contours show the same ngVLA as on the left.

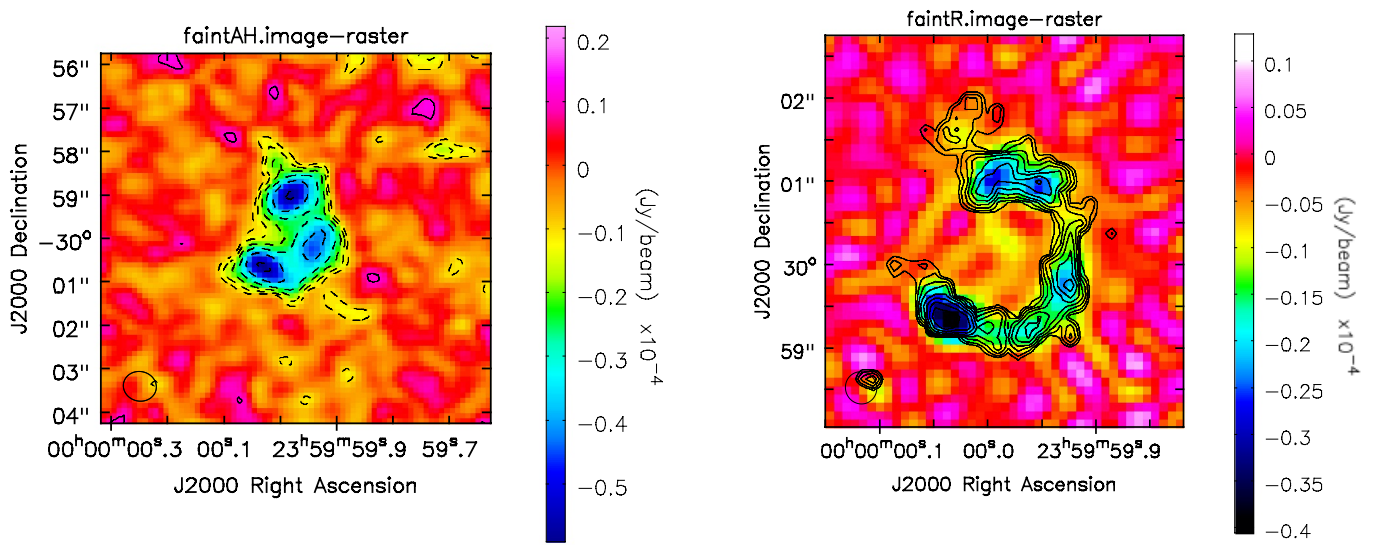


Figure 4: Left: ALMA image of the faint model at 100 GHz at $0.76'' \times 0.68''$ resolution (both contours and color scale). Right: ngVLA image of the faint model at $0.38''$ resolution (color scale). Contours are the input model.

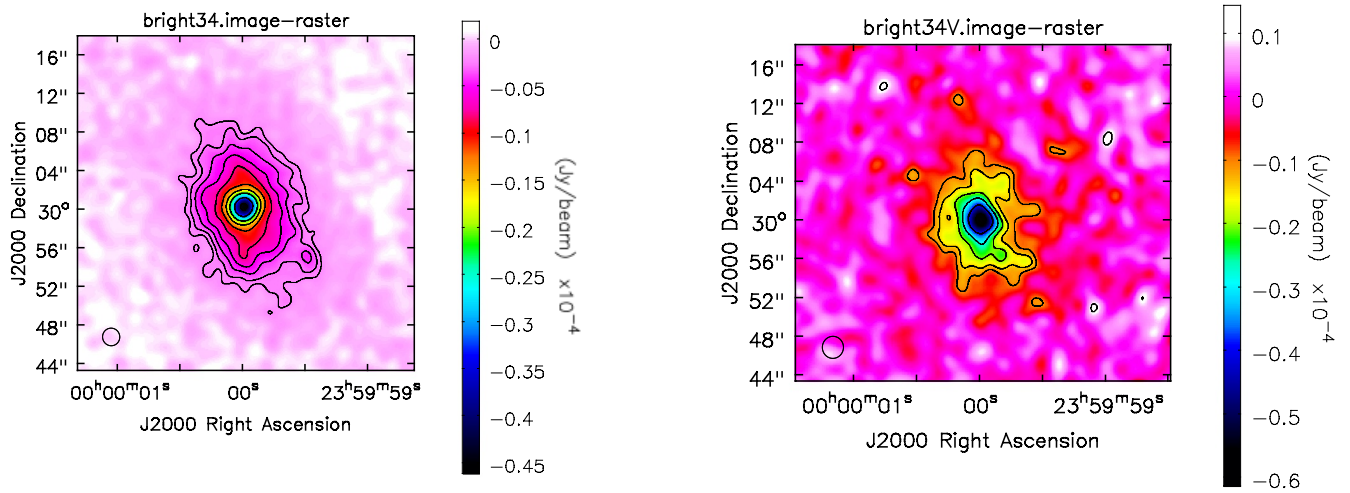


Figure 5: Left: Contours and colorscale are the ngVLA core image of the 34 GHz model at 1.8'' resolution. Right: same, but for the VLA-D configuration at 2.2'' resolution.

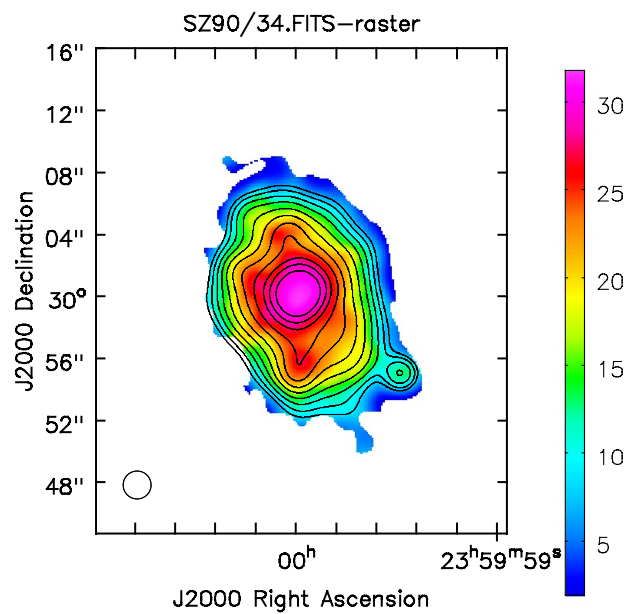


Figure 6: Contours are the ngVLA core image of the 34 GHz model. Colorscale is the ratio between the 100 GHz and 34 GHz models.

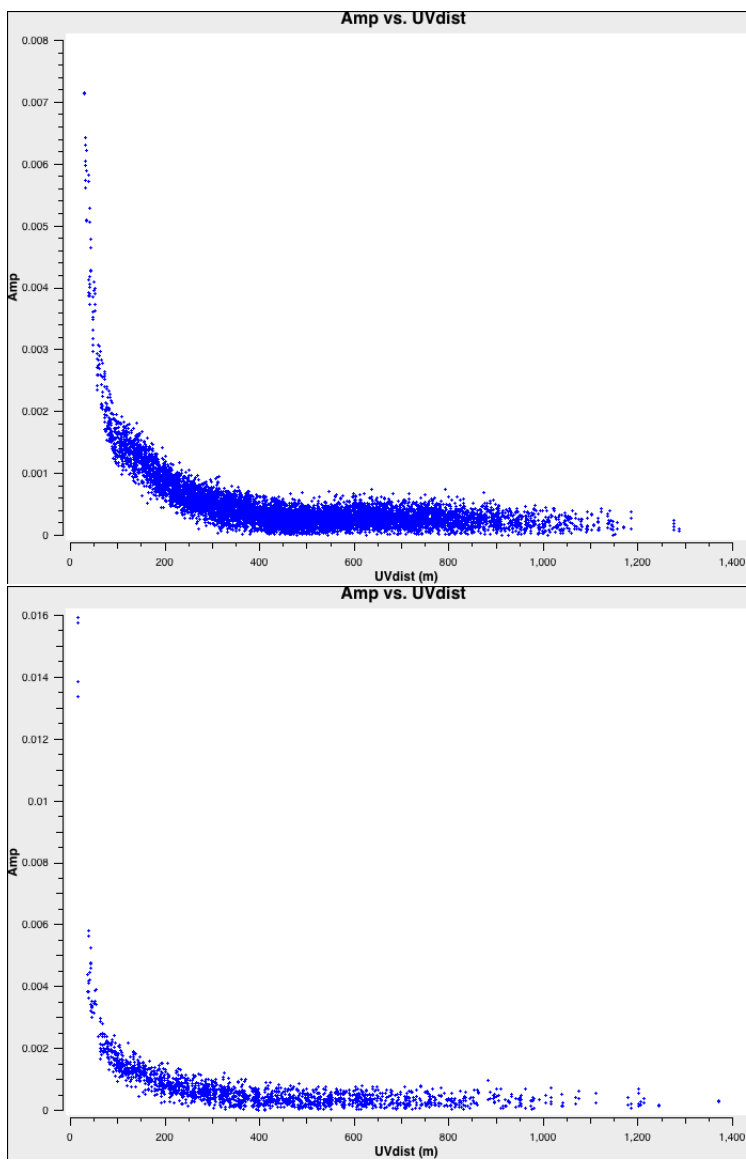


Figure 7: Top: UV plot for the ngVLA core array for the 90 GHz bright model. The Y-scale is in Jy. Bottom: same, but for the ALMA data.

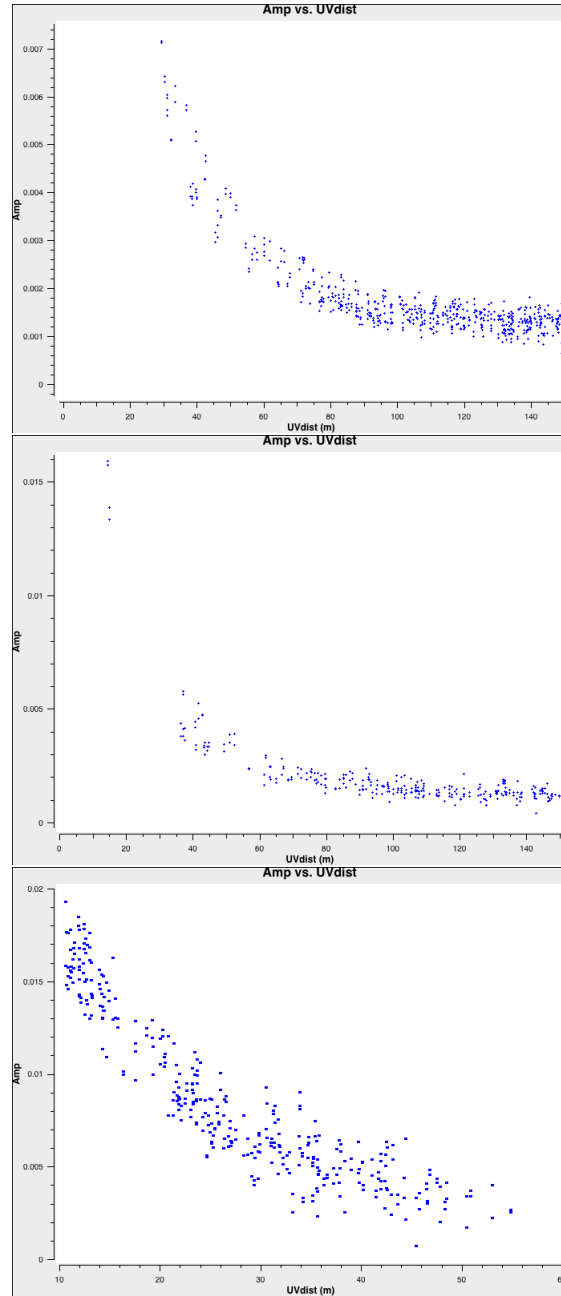


Figure 8: Top: UV plot for the ngVLA core array for the 90 GHz bright model, but just the shorter baselines to 150m. The Y-scale is in Jy. Middle: same, but for the ALMA data. Bottom: Same, but for the SBA data.